

AEC RESEARCH AND DEVELOPMENT REPORT

**TESTING OF
ENDF/B - THERMOS CROSS SECTIONS
FOR H₂O, D₂O, C, ZrH₂, (C₂H₄)_x, Be, BeO,
C₆H₆, AND UO₂**

F. J. McCROSSON

D. R. FINCH

E. C. OLSON



Savannah River Laboratory

Aiken, South Carolina

NOTICE

This report was prepared as an account of work sponsored by the United States Government. Neither the United States nor the United States Atomic Energy Commission, nor any of their employees, nor any of their contractors, subcontractors, or their employees, makes any warranty, express or implied, or assumes any legal liability or responsibility for the accuracy, completeness or usefulness of any information, apparatus, product or process disclosed, or represents that its use would not infringe privately owned rights.

Printed in the United States of America
Available from
National Technical Information Service
U. S. Department of Commerce
5285 Port Royal Road
Springfield, Virginia 22151
Price: Printed Copy \$3.00; Microfiche \$0.95

DP-1276
ENDF-158
Physics
(TID-4500, UC-34)

**TESTING OF
ENDF/B - THERMOS CROSS SECTIONS
FOR H₂O, D₂O, C, ZrH₂, (C₂H₄)_x, Be, BeO,
C₆H₆, AND UO₂**

by

F. J. McCrosson
D. R. Finch
E. C. Olson

Approved by

P. L. Roggenkamp, Research Manager
Theoretical Physics Division

October 1971

**E. I. DU PONT DE NEMOURS & COMPANY
SAVANNAH RIVER LABORATORY
AIKEN, S. C. 29801**

*CONTRACT AT(07-2)-1 WITH THE
UNITED STATES ATOMIC ENERGY COMMISSION*

ABSTRACT

Multiple temperature THERMOS multigroup cross sections were generated from the ENDF/B thermal neutron scattering data for light and heavy water, graphite, zirconium hydride, polyethylene, beryllium and beryllium oxide, benzene, and uranium dioxide using the FLANGE II processing code. No major inconsistencies were uncovered in the THERMOS cross sections, which were tested by comparisons with literature values of the total neutron cross section (σ_T), the average cosine of the scattering angle ($\bar{\mu}$), and the thermal diffusion parameters (D_0 and C).

CONTENTS

	<u>Page</u>
Introduction	7
Summary	9
Discussion	11
Kernel Generation	11
Calculating D_0 and C	15
Results	16
Water	17
Heavy Water	20
Graphite	23
Zirconium Hydride	25
Polyethylene	28
Beryllium and Beryllium Oxide	30
Benzene	36
Uranium Dioxide	38
Appendix — Scattering Kernel Library and Retrieval Routine	39
References	43

LIST OF TABLES

<u>Table</u>		<u>Page</u>
I	THERMOS Group Structure	7
II	Data Available for Each Moderator	12
III	2200 m/sec Capture Cross Sections for Moderators .	13
IV	Input Options Used in Generating Kernels	14
V	Diffusion Parameters for H ₂ O	18
VI	Diffusion Parameters for D ₂ O	21
VII	Diffusion Parameters for Graphite	25
VIII	Diffusion Parameters for ZrH ₂	27
IX	Diffusion Parameters for Polyethylene	30
X	Diffusion Parameters for Beryllium	34
XI	Diffusion Parameters for Beryllium Oxide	35
XII	Diffusion Parameters for Benzene	37

LIST OF FIGURES

<u>Figure</u>		<u>Page</u>
1	Total Neutron Cross Section for Water at 296°K . . .	17
2	$\bar{\mu}$ as a Function of Energy for Water at 296°K . . .	18
3	Temperature Dependence of the Diffusion Constant for Water	19
4	$\bar{\mu}$ as a Function of Energy for Heavy Water at 296°K	20
5	Total Neutron Cross Section for Heavy Water at 296°K	21
6	Temperature Dependence of the Diffusion Constant for Heavy Water	22
7	Total Neutron Cross Section for Graphite at 296°K .	23
8	$\bar{\mu}$ as a Function of Energy for Graphite at 296°K . .	24
9	Total Neutron Cross Section for ZrH _{1.85} at 296°K .	26
10	$\bar{\mu}$ as a Function of Energy for ZrH _{1.85} at 296°K . .	27
11	Dependency of $(\lambda - \lambda_0)/B^2$ on Geometric Buckling Calculated with ENDF/B Cross Sections for ZrH _{1.7} at 296°K	28
12	Total Neutron Cross Section for Polyethylene . . .	29
13	$\bar{\mu}$ as a Function of Energy for Polyethylene at 296°K	29
14	Total Neutron Cross Section for Beryllium at 296°K	31
15	Total Neutron Cross Section for Beryllium Oxide at 296°K	32
16	$\bar{\mu}$ as a Function of Energy for Beryllium at 296°K .	35
17	$\bar{\mu}$ as a Function of Energy for Beryllium Oxide at 296°K	33
18	$\lambda - \lambda_0$ as a Function of B^2 for Beryllium at 296°K . .	35
19	Total Neutron Cross Section for Benzene at 296°K .	36
20	$\bar{\mu}$ as a Function of Energy for Benzene at 296°K . .	37
21	Scattering Cross Section for Uranium Dioxide at 296°K	38
22	$\bar{\mu}$ as a Function of Energy for Uranium Dioxide at 296°K	38

INTRODUCTION

Integral tests of the thermal neutron scattering data for Version II ENDF/B moderators were made to verify that the Version II moderator data are free of gross errors and that FLANGE II,¹ the processing code for converting the pointwise ENDF/B data to multigroup form, is working properly. Another objective was to evaluate the overall quality of the data, but because of limited scope, the present study serves only as a starting point for such an evaluation.

In the testing procedure, the pointwise ENDF/B data were cast into the THERMOS energy group structure (Table I) with the FLANGE II code; such measurable quantities as the total neutron cross section (σ_T), the average cosine of the scattering angle ($\bar{\mu}$), the diffusion constant (D_0), and the diffusion cooling coefficient (C) were calculated; the calculations were scanned for inconsistencies, and, where possible, the calculations were compared with measured values.

TABLE I

THERMOS Group Structure

Group	Average Energy, eV	Weighting Factor	Upper Energy, eV	Group	Average Energy, eV	Weighting Factor	Upper Energy, eV
1	0.0002530	0.0005060	0.0005692	16	0.0651730	0.0089334	0.0697163
2	0.0010120	0.0010120	0.0015812	17	0.0748471	0.0104437	0.0801601
3	0.0022770	0.0015180	0.0030992	18	0.0861214	0.0121363	0.0922964
4	0.0040480	0.0020240	0.0051232	19	0.0991855	0.0140262	0.1063226
5	0.0063250	0.0025300	0.0076532	20	0.1139759	0.0155727	0.1218953
6	0.0091080	0.0030370	0.0106892	21	0.1312305	0.0190148	0.1409101
7	0.0123970	0.0035420	0.0142312	22	0.1524829	0.0236022	0.1645123
8	0.0161920	0.0040480	0.0182792	23	0.1790117	0.0296110	0.1941233
9	0.0204930	0.0045540	0.0228332	24	0.2124051	0.0373862	0.2315095
10	0.0253000	0.0050600	0.0278932	25	0.2546369	0.0473557	0.2788652
11	0.0306129	0.0055660	0.0334592	26	0.3081548	0.0600416	0.3389068
12	0.0364319	0.0060720	0.0395311	27	0.3759819	0.0760740	0.4149808
13	0.0427568	0.0065779	0.0461091	28	0.4618304	0.0962037	0.5111846
14	0.0495878	0.0070839	0.0531930	29	0.5702278	0.1213123	0.6324969
15	0.0569247	0.0075900	0.0607830	30	0.7066566	0.1524296	0.7849265

The THERMOS group structure was chosen more for its familiarity to a wide range of cross section users than its ability to represent the cross section for each material. The THERMOS energy mesh is too coarse for moderators with strong elastic components (e.g., graphite); several peaks in the energy transfer cross section may be included in a single THERMOS group for such moderators. The refinement of choosing an optimum group structure for each moderator was beyond the scope of the present study.

SUMMARY

The ENDF/B kernels for H₂O, based on the Haywood frequency spectrum,² appear to reproduce experimental scattering data more accurately than the Nelkin kernel.³ The ENDF/B kernels for D₂O appear very satisfactory, providing accuracies comparable to the Honeck model;⁴ each of these D₂O models is limited in accuracy by the use of the incoherent approximation. The ENDF/B data for H₂O and D₂O yield a weaker temperature dependence for the diffusion constant than that obtained with Radkowsky's method.⁵

The ENDF/B data for graphite give a precise representation of the highly structured scattering cross section and yield diffusion parameters similar to those obtained from the Parks kernel.⁶

At room temperature the ENDF/B kernels for zirconium hydride, beryllium, beryllium oxide, benzene, and uranium dioxide all appear satisfactory. The accuracy of the ENDF/B data at higher temperatures is less certain due to the scarcity of experimental data.

DISCUSSION

KERNEL GENERATION

THERMOS scattering kernels were generated for all the moderators listed in Table II using the FLANGE II code distributed from the Argonne Code Center in June 1969. This is an earlier version of the code described in Reference 1 and does not contain any short collision-time methods for extending the $S(\alpha,\beta,T)$ data beyond its tabulated range. Inelastic scattering, σ_{inelas} , is represented by the thermal neutron scattering law $S(\alpha,\beta,T)$, i.e.,

$$\sigma_{\text{inelas}}(E \rightarrow E', \mu, T) = \frac{N_0 \sigma_b}{4\pi T} \left(\frac{E'}{E}\right)^{\frac{1}{2}} e^{-\beta/2} S(\alpha, \beta, T)$$

where

E = incident neutron energy

E' = secondary neutron energy

μ = cosine of the scattering angle

T = moderator temperature

N_0 = molecular density

σ_b = bound atom scattering cross section

$\beta = (E' - E)/(kT)$

$\alpha = (E' + E - 2\mu\sqrt{EE'})/(AkT)$

A = atomic mass of molecule

k = Boltzmann's constant

Table II also lists the ENDF/B tape labels and the type of data available on the tapes, i.e., whether scattering law data, Legendre moments for elastic scattering, or neutron capture cross sections are available.

TABLE II
Data Available for Each Moderator

Material	MAT ^a	ZA ^b	ENDF/B Tape Label	S(α, β, T)	$\sigma_{\ell_{\text{elast}}}^c$	σ_{γ}^d
H ₂ O	1002	100.0	6007	x		x
D ₂ O	1004	101.0	6007	x		x
(C ₂ H ₄) _x	1011	205.0	7005	x		x
Be	1064	4009.0	5005	x	x	x
C	1065	6000.0	7005	x	x	x
C ₆ H ₆	1095	106.0	9001	x	x	x
Zr in ZrH _x	1096	203.0	8503	x	x	x
H in ZrH _x	1097	230.0	8503	x	x	x
UO ₂	1098	207.0	9501	x	x	
BeO	1099	200.0	9001	x	x	x

- a. MAT is the unique ENDF/B code number used to identify a specific cross section evaluation for a given material (Reference 1).
- b. ZA is the ENDF/B code number for designating materials (Reference 1).
- c. $\sigma_{\ell_{\text{elast}}}$ = Legendre moment for elastic scattering
- d. σ_{γ} = radiative capture cross section.

Because the ENDF/B 2200 m/sec neutron capture cross sections for these moderators have not been widely distributed, these are listed in Table III. The capture cross sections follow a $1/\sqrt{E}$ energy dependence based on these values. For convenience, the THERMOS kernels have been made into a two-volume library on magnetic tape from which data can be printed and/or punched using a specially prepared retrieval routine. Group-structure information for the kernels is included in each volume of the library, which, together with the retrieval routine, is available from the Argonne Code Center. The input for the retrieval routine and the structure of the library are described in the Appendix.

TABLE III

2200 m/sec Capture Cross Sections for Moderators

<u>Material</u>	<u>MAT</u>	<u>σ_γ at 0.0253 eV</u>	
H ₂ O	1002	664.0	mb
D ₂ O	1004	0.92	mb
(C ₂ H ₄) _x	1011	667.4	mb
Be	1064	10.0	mb
C	1065	3.4	mb
C ₆ H ₆	1095	2.0124	b
Zr in ZrH _x	1096	185.0	mb ^a
H in ZrH _x	1097	332.0	mb ^a
BeO	1099	10.0	mb

a. millibarns/atom; other cross sections are millibarns/molecule, except C₆H₆.

In generating the scattering kernels, the following principles were employed:

- Inelastic Legendre cross sections were obtained by accurate numerical integration of the $S(\alpha, \beta, T)$ data.
- Group-averaged elastic Legendre cross sections were computed when data existed in ENDF/B Files 3 and 4.
- Kernels were normalized to the exact total Legendre scattering cross section defined as the sum of the elastic and inelastic components.

The indices used to specify the FLANGE II options are shown in Table IV (see Ref. 1 for notation).

TABLE IV

Input Options Used in Generating Kernels

<u>Material</u>	<u>MAT</u>	<u>LELAS</u>	<u>LPELAS</u>	<u>LTSL</u>
H ₂ O	1002	0	0	4
D ₂ O	1004	0	0	4
(C ₂ H ₄) _x	1011	0	0	4
Be	1064	1	-2	5
C	1065	1	-2	5
C ₆ H ₆	1095	1	-2	5
Zr in ZrH _x	1096	1	-2	5
H in ZrH _x	1097	1	-2	5
UO ₂	1098	1	-2	5
BeO	1099	1	-2	5

The following indices were the same for all kernels except material 1098 (for 1098, the indices with asterisks (*) were zero):

*LABS = 1	*LPABS = -2
LPDD = 0	LPFP = 0
LFISS = 0	LPFISS = 0
*LTOT = 2	*LPTOT = -1
LINEL = 3	LPINEL = -1
LSCAT = 2	LPSC = -1
LPTR = -2	LPTSL = 2

CALCULATING D_0 AND C

The diffusion parameters D_0 and C for the THERMOS scattering kernels were obtained using the PIDLE code (Proper Integration of the Diffusion Length Equation). PIDLE is a thoroughly tested in-house code which computes the inverse diffusion length, κ , of the diffusion length experiment. In PIDLE, it is assumed the spatial dependence of the flux in slab geometry can be represented by a single Fourier component

$$\phi(z, E, \mu) = \phi(E, \mu) e^{-\kappa z} \quad (1)$$

where z , E , and μ represent the position, energy, and direction coordinates.

The energy-angle variation, $\phi(E, \mu)$, is obtained from the eigenvalue equation,

$$\begin{aligned} & \left[\sum_a(E) - \kappa \mu \right] \phi(E, \mu) \\ &= \int_{-1}^1 d\mu' \int_0^\infty dE' \sum_s(E' \rightarrow E, \mu_0) \phi(E', \mu') - \sum_s(E) \phi(E, \mu) \end{aligned} \quad (2)$$

which is analyzed in a straightforward way using the spherical harmonics method outlined by Honeck.⁷ In the above equation, \sum_a and \sum_s are the absorption and scattering cross sections, $\sum_s(E' \rightarrow E, \mu_0)$ is the scattering kernel, and μ_0 is the cosine of the angle of scatter. The mathematical relationship between the static and pulsed neutron experiments is used to derive D_0 and C.

For the present study, the total absorption cross section of the system (moderator plus added absorber) was assumed to vary inversely with neutron speed. Anisotropy in the scattering kernel was represented by a P_3 Legendre expansion. For each moderator, κ was computed for eleven different absorption cross sections, $A = \sum_a(kT)$, where kT = thermal energy. The eigenvalues were then fitted to a three-term series in A,

$$\frac{\kappa^2}{A} = \alpha_1 - \alpha_2 A + \alpha_3 A^2 \quad (3)$$

where the expansion coefficients, α , were determined by conventional least squares analysis. Generally, the eleven values of A were chosen to be equally spaced over an interval symmetric with

respect to the origin. However, some exceptions to this practice will be noted in subsequent sections. Following the theorems of Corngold,⁸ the limits of the interval were always chosen small enough to ensure physically meaningful eigenvalues. Whereas the positive segment of the interval corresponds to different poison concentrations in the moderator for the diffusion length experiment, the negative segment can be identified with the pulsed neutron experiment through the relations

$$-v_0A \leftrightarrow \lambda - \lambda_0 \quad (4a)$$

$$-k^2 \leftrightarrow B^2 \quad (4b)$$

The symbol v_0 is the speed of a neutron at thermal energy kT , B^2 is the geometric buckling of the pulsed neutron experiment, λ is the decay constant, and λ_0 is the absorption probability, $v \int_a^\infty \Sigma_a(E)$. The diffusion parameters D_0 and C , which are usually associated with the pulsed neutron experiment, and the expansion

$$\lambda = \lambda_0 + D_0 B^2 - C B^4 \quad (5)$$

were then computed using the relations

$$D_0 = v_0/\alpha_1 \quad (6a)$$

$$C = v_0\alpha_2/\alpha_1^3 \quad (6b)$$

These relations have been derived by Honeck⁷ by combining Equations 3 through 5.

RESULTS

This section outlines the results of the data testing for the materials in Table II. Only the graphs for σ_T and $\bar{\mu}$ versus energy at 296°K have been included here since they are generally indicative of the quality of the data at other temperatures. To display all the structure of the total cross section for moderators with strong elastic scattering components (graphite, zirconium hydride, beryllium, and beryllium oxide), the elastic scattering component was obtained directly from the ENDF/B pointwise data, and only the absorption and smooth inelastic scattering cross sections were taken from the 30-group FLANGE II output. In contrast, some of the structure of $\bar{\mu}$ for these moderators is not evident in the graphs, since for simplicity both the elastic and inelastic contributions were obtained from the FLANGE II output.

Water

Scattering kernels were tested and found satisfactory at each of the following temperatures: 296°, 350°, 400°, 450°, 500°, 600°, 800°, and 1000°K.

Excellent agreement between the 30-group FLANGE II output at 296°K and the total neutron cross section measurements of Russell, et al.⁹ is shown in Figure 1. For $\bar{\mu}$ at 296°K (Figure 2), the ENDF/B values are consistently higher than those obtained by Beyster,¹⁰ but lower than those obtained by Nelkin.³ Thus, the ENDF/B data based on Haywood's frequency spectrum² is expected to yield smaller values for the thermal diffusion constant D_0 than that from the Nelkin model. Table V compares the results of the present PIDLE calculations to calculations by Honeck⁷ using the Nelkin model and also to some experimental determinations.

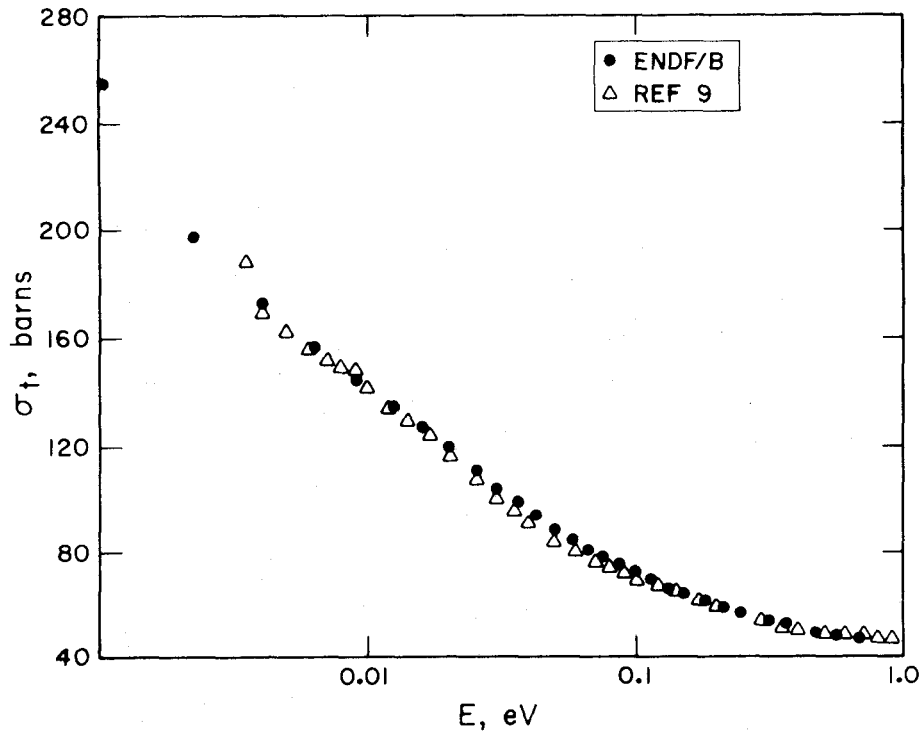


FIGURE 1 Total Neutron Cross Section for Water at 296°K

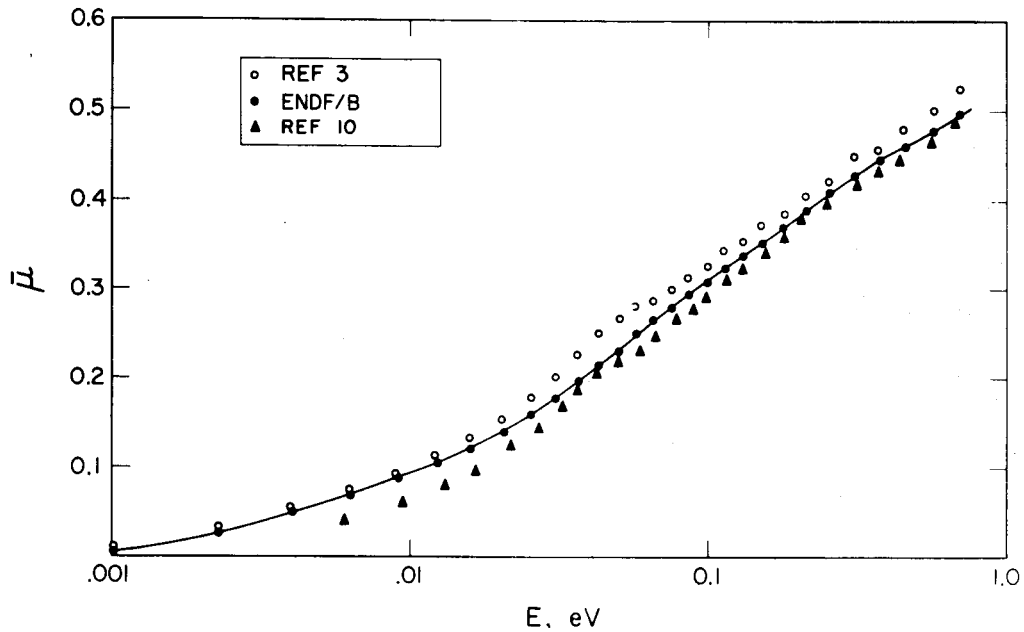


FIGURE 2 \bar{u} as a Function of Energy for Water at 296°K

TABLE V
Diffusion Parameters for H₂O
($\rho = 1.0 \text{ g/cm}^3$)

Method	T, °K	$D_0, 10^4 \text{ cm}^2/\text{sec}^\alpha$	$C, 10^3 \text{ cm}^4/\text{sec}$
ENDF/B Data	296	3.49	3.37
	350	4.07	3.88
	400	4.60	4.27
	450	5.10	4.71
	500	5.60	5.09
	600	6.56	5.85
	800	8.35	7.25
	1000	10.02	8.58
Reference 7	296	3.75	3.13
Reference 11	296	3.585 ± 0.01	2.90 ± 0.35
Reference 12	296	3.57 ± 0.04	3.31 ± 0.15
Reference 13	296	3.562 ± 0.023	2.80 ± 0.26

α . In all tables, the number is to be multiplied by the power of ten indicated in the column heading.

The ENDF/B data yields a weaker temperature dependence for D_0 (Figure 3) than that derived from Reference 5. In making this comparison, D_0 for the Radkowsky method was computed using the empirical formula in Reference 14.

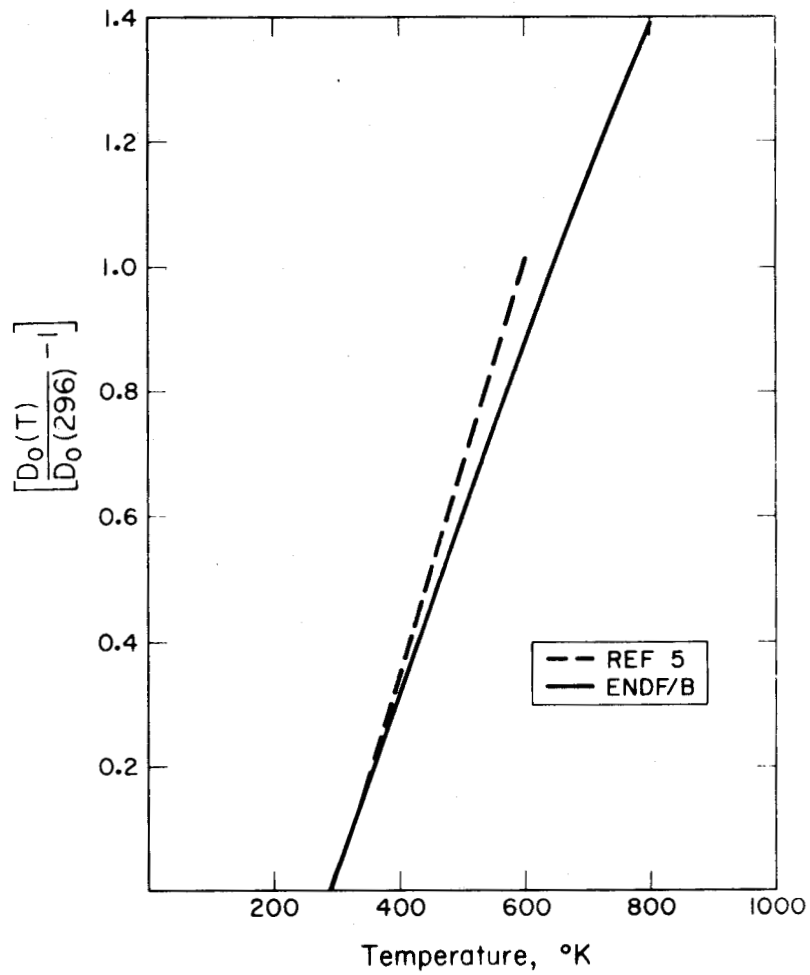


FIGURE 3 Temperature Dependence of the Diffusion Constant for Water

Heavy Water

THERMOS scattering kernels were generated and tested for the same temperatures as those of water kernels. When integral parameters were tested, minor differences between these values and experimental values were found, but these can be attributed to the incoherent approximation which was used to generate the $S(\alpha, \beta, T)$ data. For example, most of the discrepancy between the FLANGE II values and the experimental values for $\bar{\mu}$, shown in Figure 4, can be attributed to coherent scattering, which is not accounted for in the present ENDF/B model for D_2O . In Figure 5, the agreement is quite good between the FLANGE II values and the experimental values of σ_T at $296^\circ K$ due to the fortuitous cancellation of the interference scattering effects. Table VI shows that the diffusion parameters D_0 and C are in reasonable agreement with experiment. Honeck's calculations using his incoherent scattering model^{4,7} appear in somewhat better agreement with experiment.

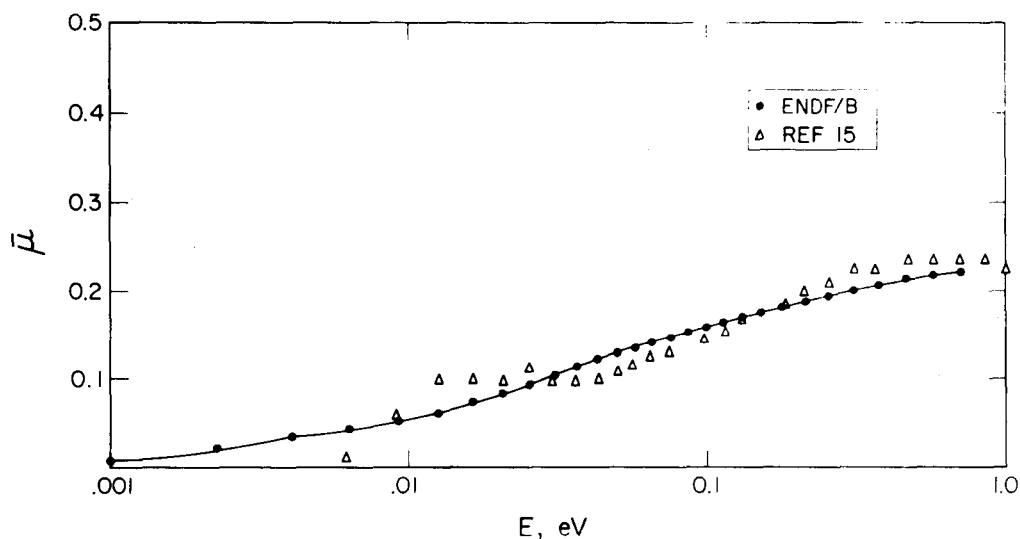


FIGURE 4 $\bar{\mu}$ as a Function of Energy for Heavy Water at $296^\circ K$

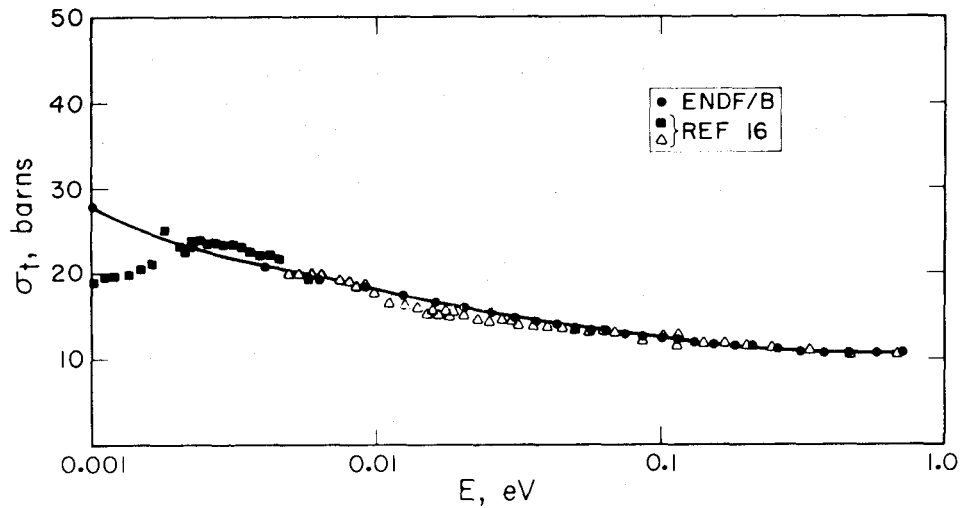


FIGURE 5 Total Neutron Cross Section for Heavy Water at 296°K

TABLE VI

Diffusion Parameters for D₂O
($\rho = 1.1054 \text{ g/cm}^3$)

Method	T, °K	D ₀ , 10 ⁵ cm ² /sec	C, 10 ⁵ cm ⁴ /sec
ENDF/B Data	296	1.98	5.76
	350	2.23	6.03
	400	2.43	6.30
	450	2.62	6.55
	500	2.81	6.77
	600	3.16	7.21
	800	3.80	7.94
	1000	4.36	8.42
Reference 7	296	2.07	5.13
Reference 17	296	2.08 ±0.05	3.72 ±0.50
Reference 12	296	2.09 ±0.02	6.6 ±0.3
Reference 18	297	2.045 ±0.044	4.706 ±0.381
Reference 19	296	2.00 ±0.01	5.25 ±0.25

Figure 6 compares the temperature dependence of D_0 calculated from ENDF/B data with the empirical formula in Reference 14. Baumann's¹⁴ formula was obtained using Radkowsky's method⁵ for determining the transport cross section as modified by Spielberg.²⁰

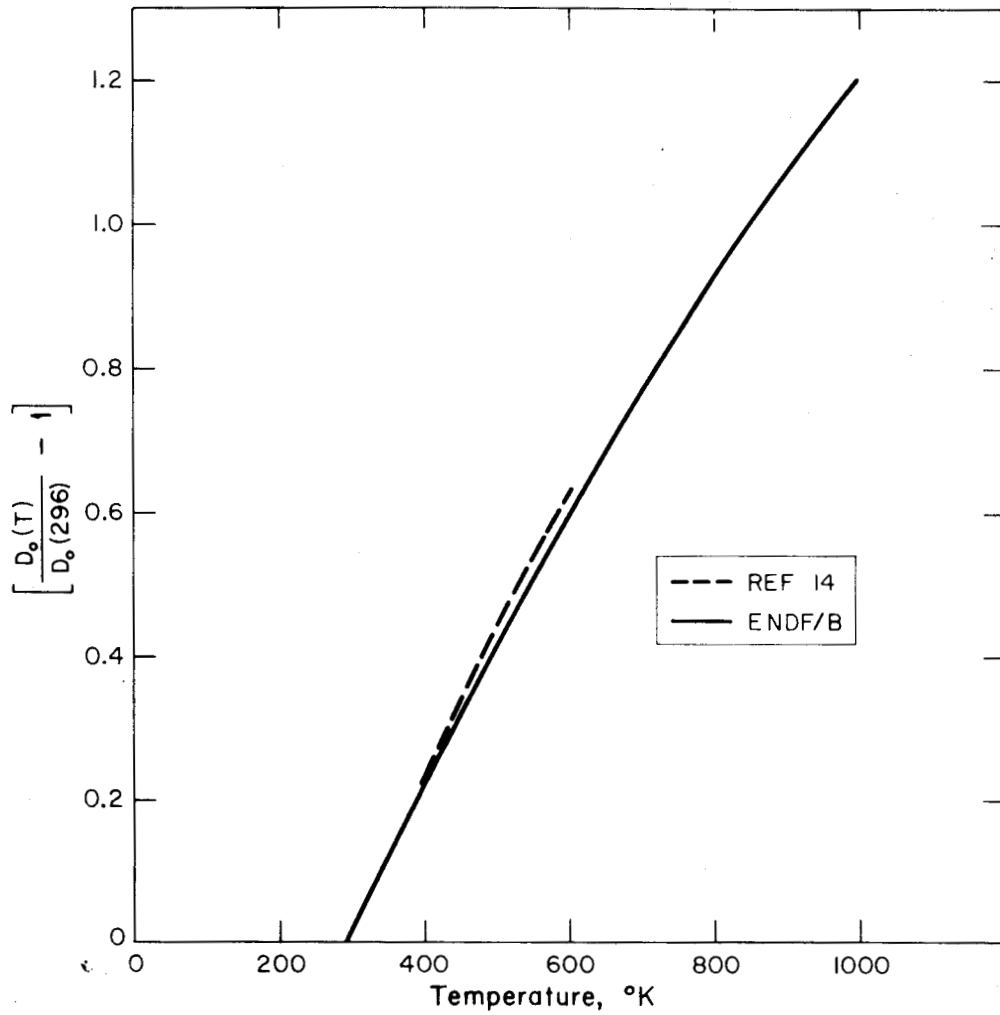


FIGURE 6 Temperature Dependence of the Diffusion Constant for Heavy Water

Graphite

Scattering kernels were tested and found satisfactory at each of the following temperatures: 296°, 400°, 500°, 600°, 700°, 800°, 1000°, 1200°, 1600°, and 2000°K.

Figure 7 indicates that the ENDF/B data for 296°K yield a total cross section which is in excellent agreement with the experimental data of Walton²¹ above the Bragg peak at 0.002 eV. Below 0.002 eV, the ENDF/B data falls somewhat below the room temperature measurements reported in Reference 16. (Walton's measurements appear to be too high below the Bragg peak.) Only the 30 group-averaged values from the FLANGE II output were used in plotting $\bar{\mu}$; hence, the lack of resolution is seen in Figure 8.

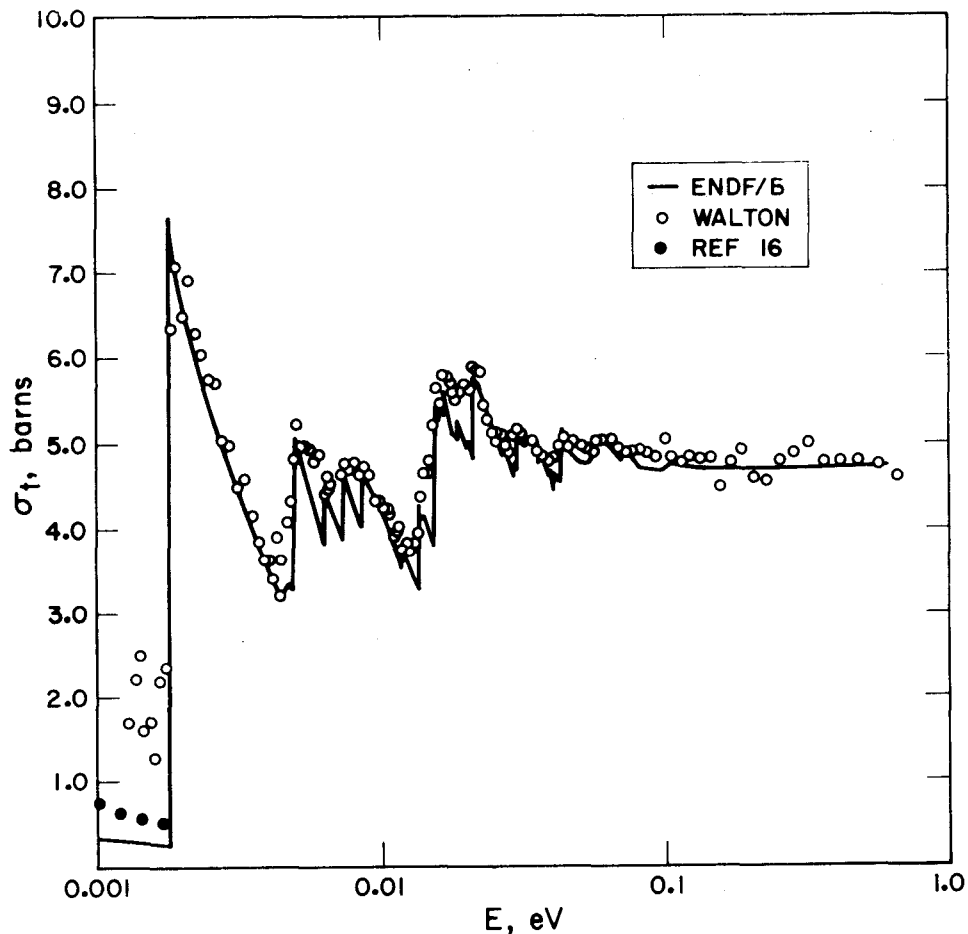


FIGURE 7 Total Neutron Cross Section for Graphite at 296°K

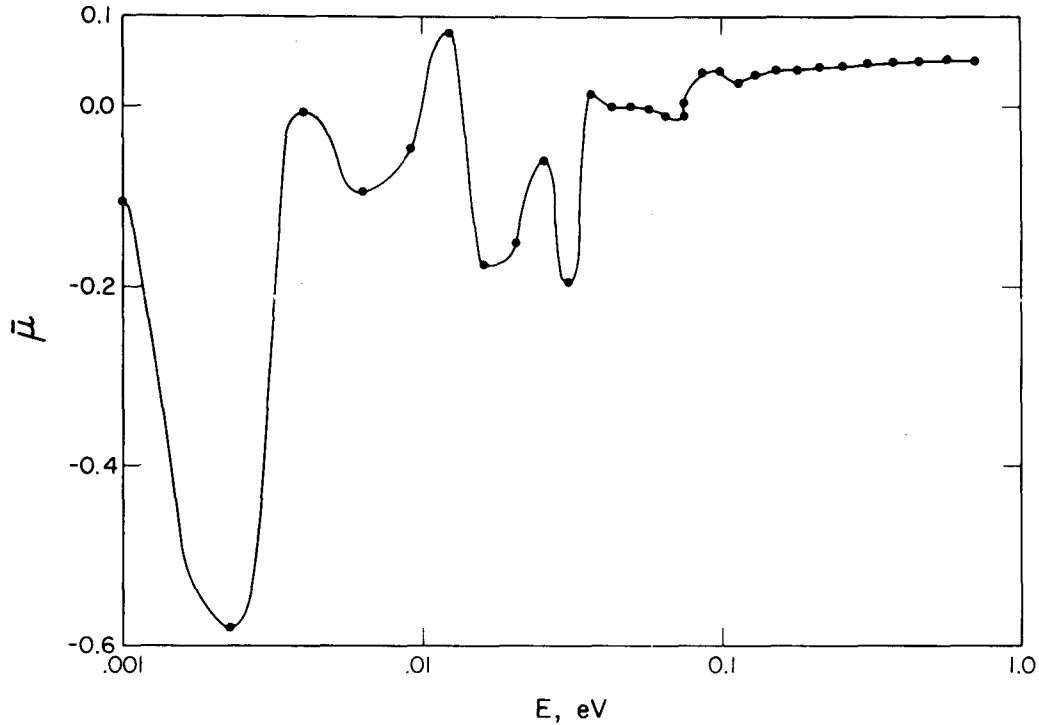


FIGURE 8 $\bar{\mu}$ as a Function of Energy for Graphite at 296°K

The PIDLE results for the diffusion parameters D_0 and C in Equation 5 are tabulated in Table VII. These parameters correspond to a least squares fit of λ versus B^2 over the buckling interval $0.0 < B^2 < 0.001 \text{ cm}^{-2}$. In spite of differences in the buckling intervals used in the various least squares analyses,²² the ENDF/B results at 296°K are in good agreement (Table VII) with the calculations of Honeck⁷ who used the Parks kernel,⁶ and the experimental determination of Starr and Price.²³ The ENDF/B results are also in good agreement with the experimental determinations of Takahashi and Sumita,²⁴ who used the sinusoidally modulated neutron source technique²⁵ over the frequency range 0.0 to 1.89 rads/sec. The ENDF/B data yield a minimum scattering cross section of 0.36 barn at 0.00065 eV. Hence, in accordance with Corngold's theorems,⁸ the ENDF/B scattering cross section implies that pulsed neutron experiments for room temperature graphite with $\rho = 1.6 \text{ g/cm}^3$ cannot give meaningful values for $\lambda - \lambda_0$ above 1030 sec^{-1} . Based on Equation 5 and the ENDF/B diffusion parameters in Table VII, this limit corresponds to a buckling of 0.005 cm^{-2} , i.e., ENDF/B implies that meaningful decay constants cannot be obtained outside the buckling range $0.0 < B^2 < 0.005 \text{ cm}^{-2}$. No attempt was made, therefore, to extend the ENDF/B calculations for D_0 and C to the larger bucklings studied by both Honeck⁷ and Starr and Price.²³

TABLE VII
Diffusion Parameters for Graphite
($\rho = 1.6 \text{ g/cm}^3$)

Method	B^2 Interval, cm^{-2}	T, °K	D_0 , $10^5 \text{ cm}^2/\text{sec}$	C, $10^5 \text{ cm}^2/\text{sec}$
ENDF/B Data	0.0< B^2 <0.001	296	2.18	24.6
		400	2.51	25.7
		500	2.82	22.9
		600	3.10	21.2
		700	3.37	21.1
		800	3.61	20.4
		1000	4.03	18.5
		1200	4.42	17.6
		1600	4.95	14.9
	2000	5.40	13.6	
Reference 7	0.0< B^2 <0.015	296	2.18	24.6
Reference 23	0.0076<	296	2.14 \pm 0.01	39 \pm 3
	B^2 <0.0189			
Reference 24		296	2.16 \pm 0.02	28 \pm 3

Zirconium Hydride

In the present study, THERMOS scattering kernels for Zr and H as bound in ZrH_x were generated from ENDF/B Tape 8503 at the following temperatures: 296°, 400°, 500°, 600°, 700°, 800°, 1000°, and 1200°K. The integral tests revealed no major deficiencies in these kernels.*

The total cross section for $\text{ZrH}_{1.85}$ at 296°K is shown in Figure 9, where excellent agreement is seen between the FLANGE II output and the experimental determinations. The data of Reference 26 was chosen over that of Reference 27 above 0.02 eV because the latter exhibited anomalies which could be due to the presence of room return neutrons.

* An earlier ENDF/B distribution of scattering law data (Tape 8501) contained an error in the 600°K data for Zr as bound in ZrH_x .

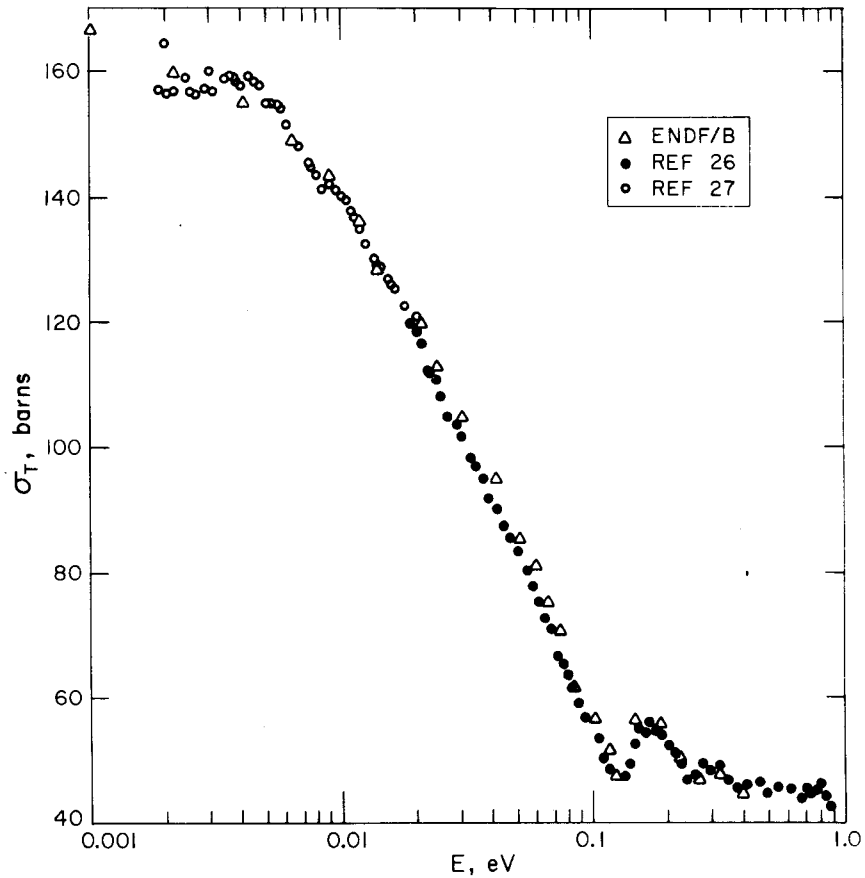


FIGURE 9 Total Neutron Cross Section for $ZrH_{1.85}$ at $296^{\circ}K$

Figure 10 shows that the agreement between FLANGE II and the experimental determination of $\bar{\mu}$ at $296^{\circ}K$ is not very satisfactory. The disparity in the oscillatory region above 0.08 eV is most likely due to the simple frequency spectrum used to generate the pointwise ENDF/B data, rather than to errors in the conversion of the ENDF/B data to multigroup form or to deficiencies in the experimental data. (See, for example, the data presented by W Gläser.²⁸)

Table VIII indicates that the diffusion parameters obtained using ENDF/B data are in good agreement with those computed by Reichardt using his Gaussian model,²⁹ and also with those determined experimentally by Meadows and Whalen.³⁰ The striking difference between the $ZrH_{1.7}$ diffusion parameters of the Reichardt study and those of the Meadows and Whalen study (Figure 11) is caused by the different buckling intervals analyzed in these investigations. Whereas the use of Equation 5 to determine D_0 and C in the pulsed neutron experiment assumes that $(\lambda - \lambda_0)/B^2$ varies linearly with buckling, the PIDLE results using ENDF/B cross sections demonstrate that $(\lambda - \lambda_0)/B^2$ for $ZrH_{1.7}$ has a pronounced nonlinear dependence on buckling in the range $0.0 < B^2 < 0.10 \text{ cm}^{-2}$.

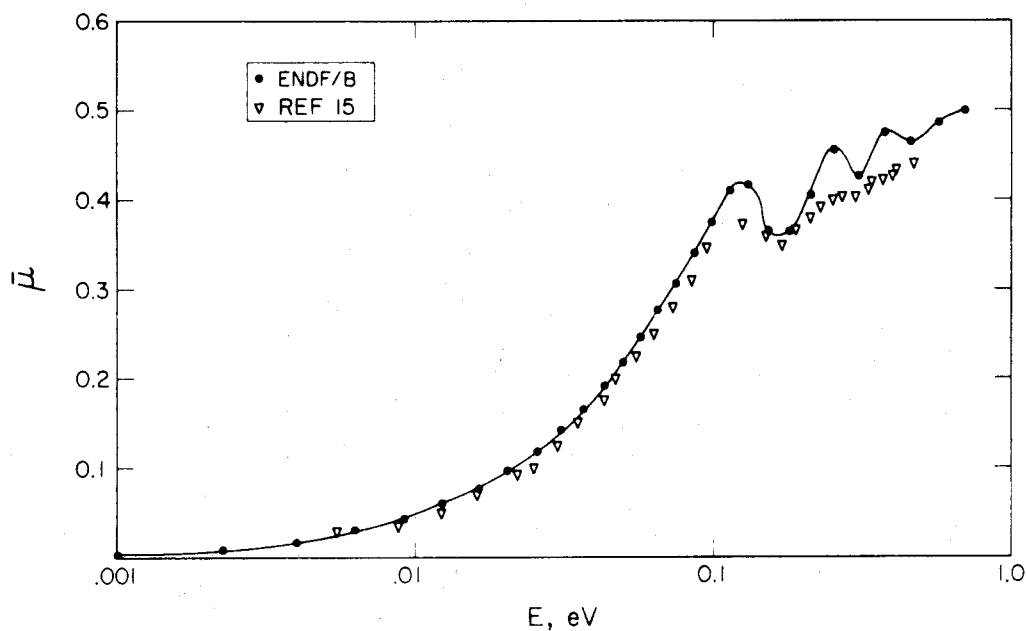


FIGURE 10 $\bar{\mu}$ as a Function of Energy for $\text{ZrH}_{1.85}$ at 296°K

TABLE VIII

Diffusion Parameters for ZrH_2
 ($\rho = 5.61 \text{ g/cm}^3$)

Method	B^2 Interval	$T, ^\circ\text{K}$	$D_0, 10^4 \text{ cm}^2/\text{sec}$	$C, 10^4 \text{ cm}^4/\text{sec}$
ENDF/B Data	$-0.01 < \Sigma_a < 0.01 \text{ cm}^{-1}$	296	3.38	5.21
		400	4.72	4.00
		500	5.89	2.94
		600	6.90	2.40
		700	7.86	1.70
		800	8.68	1.35
		1000	10.1	0.962
		1200	11.3	0.768
ENDF/B Data ^a	$0.0 < B^2 < 0.03 \text{ cm}^{-2}$	296	6.21	31.3
Reference 29		296	6.39	34.6
ENDF/B Data ^a	$0.03 < B^2 < 0.11 \text{ cm}^{-2}$	296	5.75	15.2
Reference 30		296	5.79 ± 0.32	21.2 ± 3.5

^a. $\text{ZrH}_{1.7}$, $\rho = 3.48 \text{ g/cm}^3$

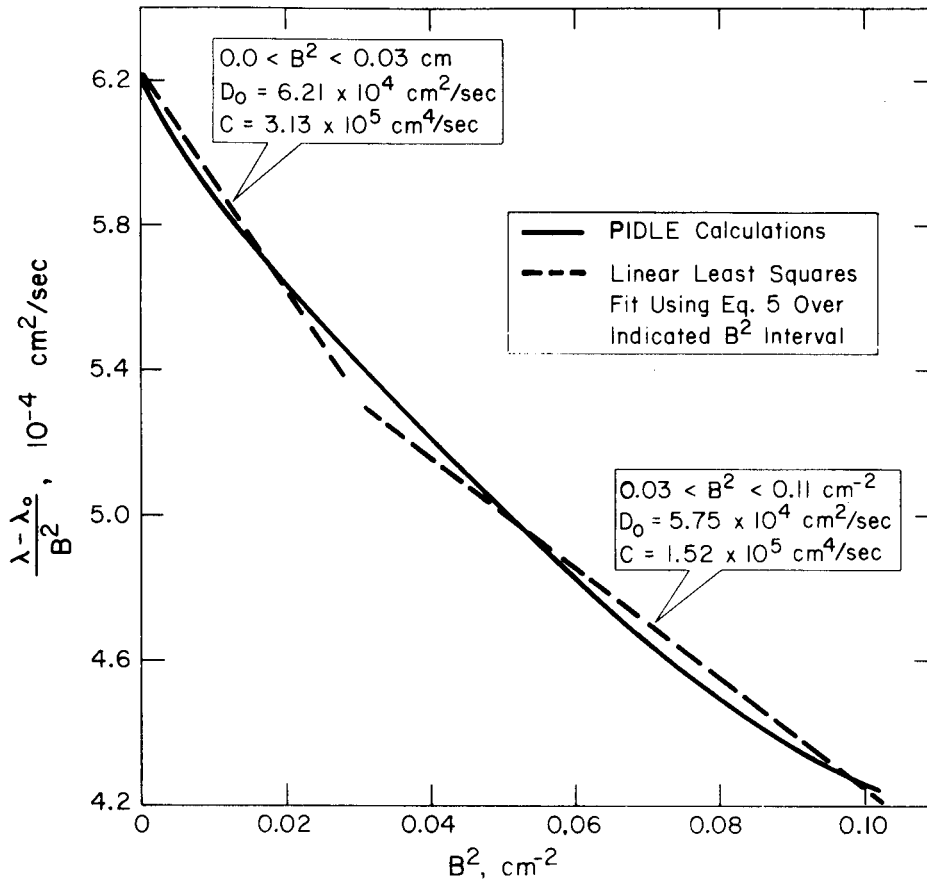


FIGURE 11 Dependency of $(\lambda - \lambda_0)/B^2$ on Geometric Buckling Calculated with ENDF/B Cross Sections for $ZrH_{1.7}$ at 296°K

Polyethylene

THERMOS scattering kernels were tested and found to be satisfactory at 296° and 350°K. The FLANGE II results for σ_T at 296°K, in Figure 12, are in good agreement with Armstrong's experimental findings.³¹

The FLANGE II values for $\bar{\mu}$ (Figure 13) are consistently higher than the experimental determinations.³²

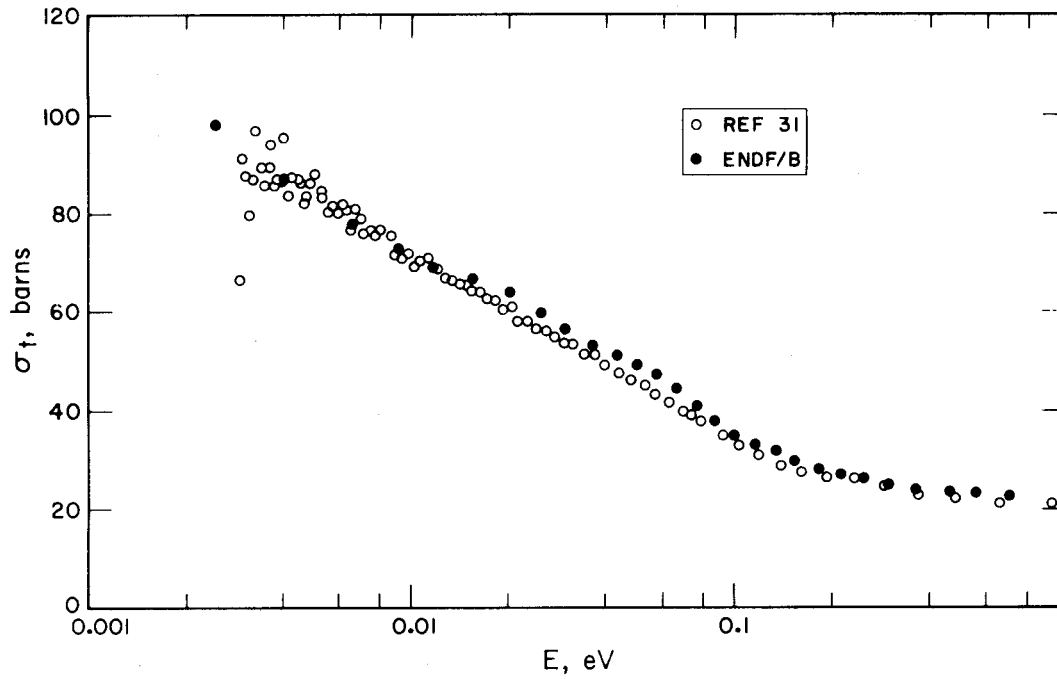


FIGURE 12 Total Neutron Cross Section for Polyethylene

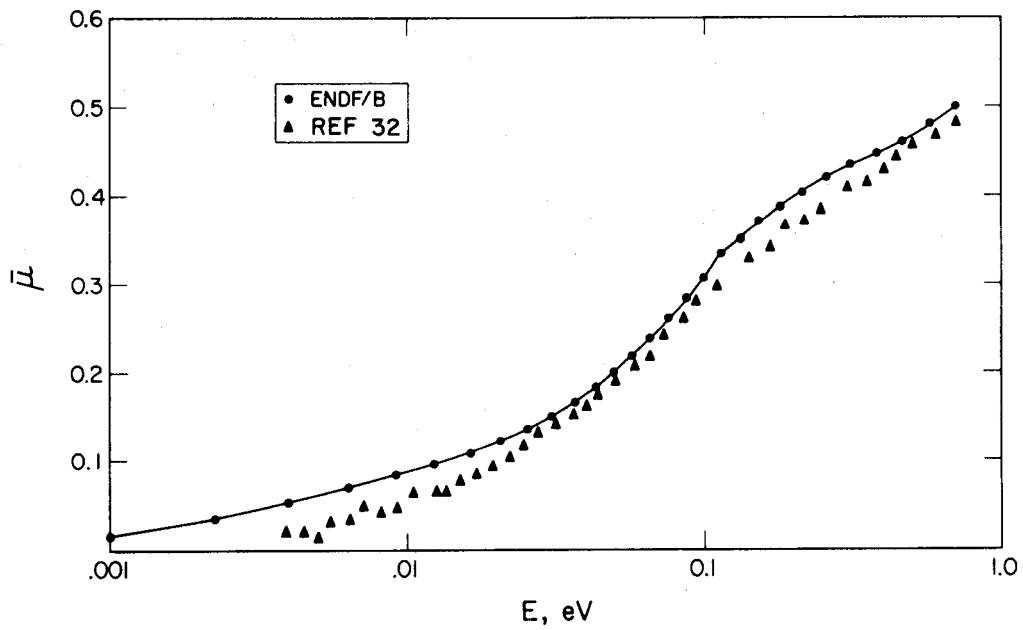


FIGURE 13 $\bar{\mu}$ as a Function of Energy for Polyethylene at 296°K

The calculated diffusion parameters (Table IX) are in excellent agreement with experiment.

TABLE IX
Diffusion Parameters for Polyethylene
($\rho = 0.918 \text{ g/cm}^3$)

<u>Method</u>	<u>T, °K</u>	<u>D₀, 10⁴ cm²/sec</u>	<u>C, 10⁴ cm⁴/sec</u>
ENDF/B Data	296	2.61	0.264
	350	3.11	0.337
Reference 33	296	2.65 ±0.06	0.300 ±0.08

Beryllium and Beryllium Oxide

Scattering kernels were tested and found satisfactory at each of the following temperatures: 296°, 400°, 500°, 600°, 700°, 800°, 1000°, and 1200°K. The ENDF/B pointwise data for the total cross section of beryllium at 296°K are in excellent agreement with the measurements reported in Reference 16 (Figure 14). Similarly, the ENDF/B data for σ_T at 296°K for beryllium oxide are in excellent agreement with the 1947 measurements of Fermi, et al.³⁴ (Figure 15). The group-averaged FLANGE II output for $\bar{\mu}$ for beryllium and beryllium oxide at 296°K are shown in Figures 16 and 17; no experimental determinations were found in the literature.

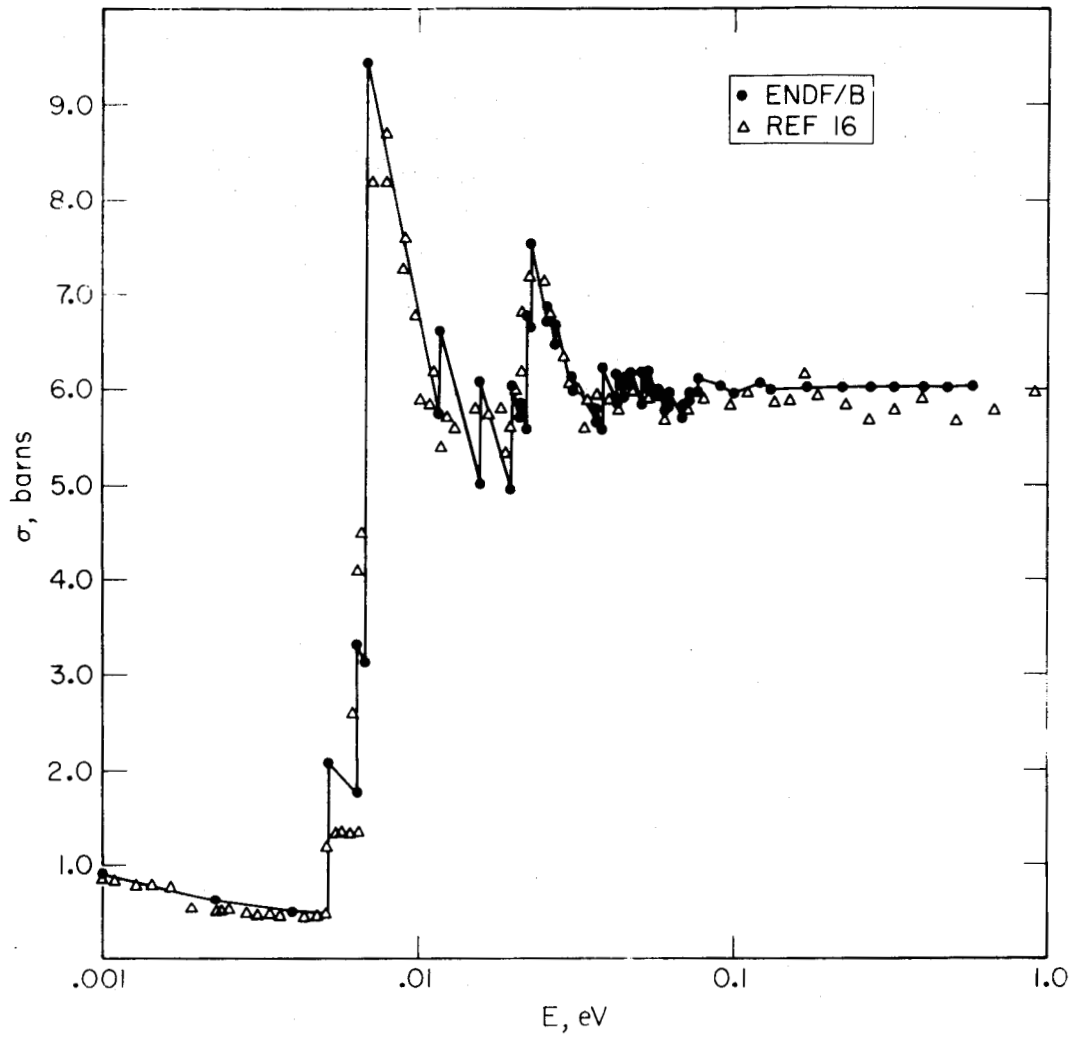


FIGURE 14 Total Neutron Cross Section for Beryllium at 296°K

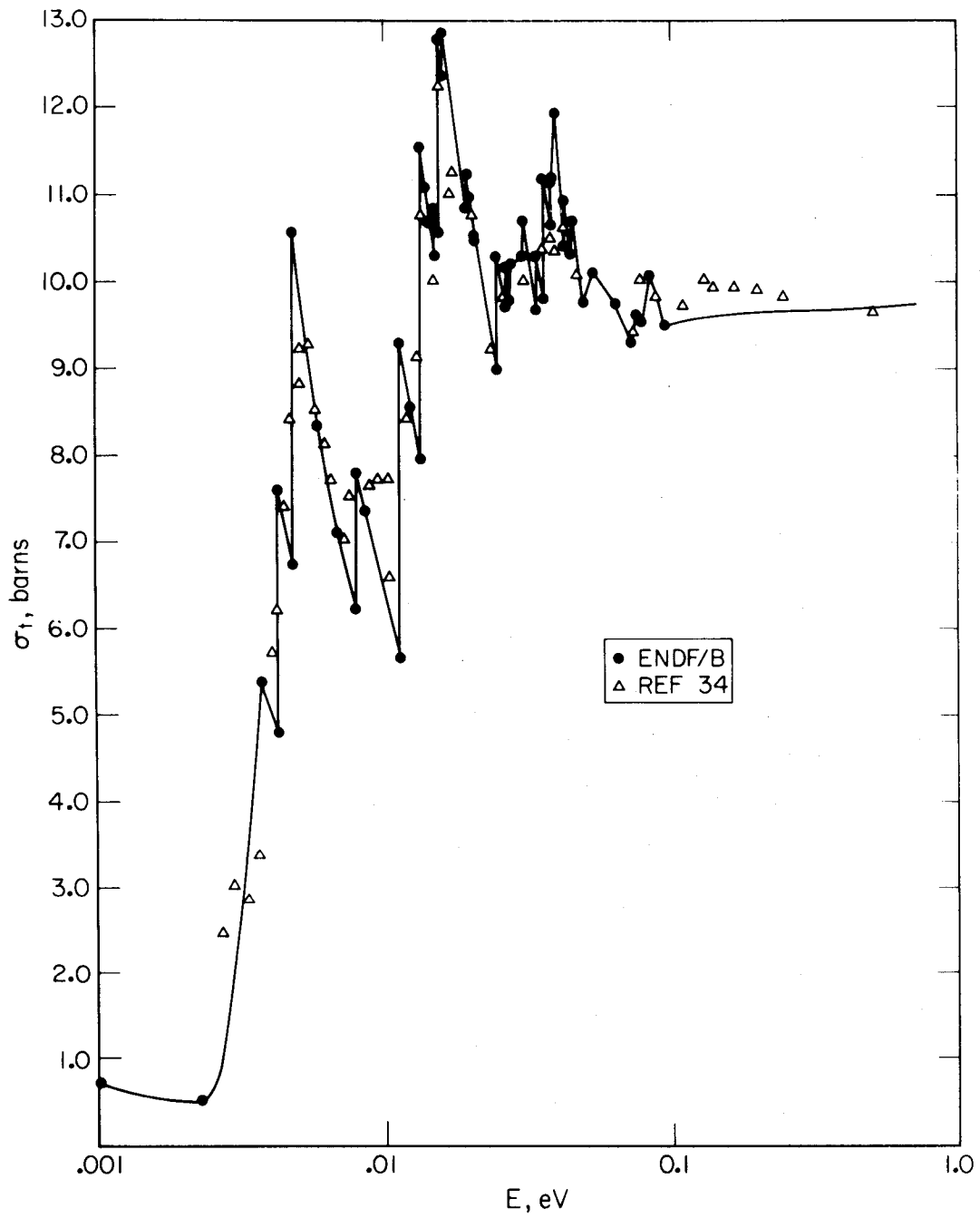


FIGURE 15 Total Neutron Cross Section for Beryllium Oxide at 296°K

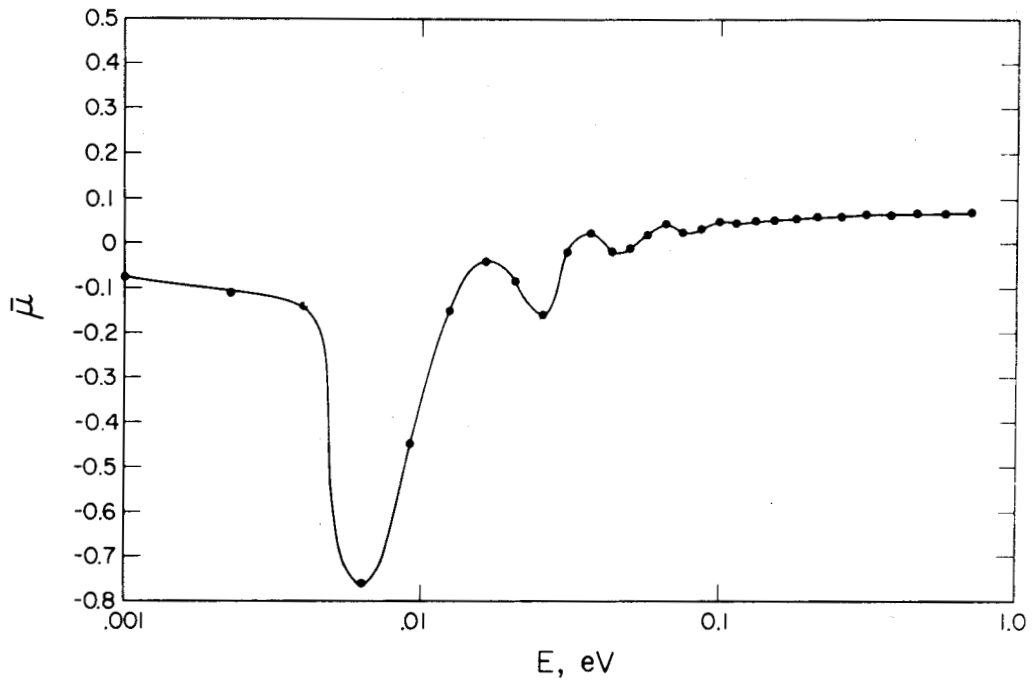


FIGURE 16 $\bar{\mu}$ as a Function of Energy for Beryllium at 296°K

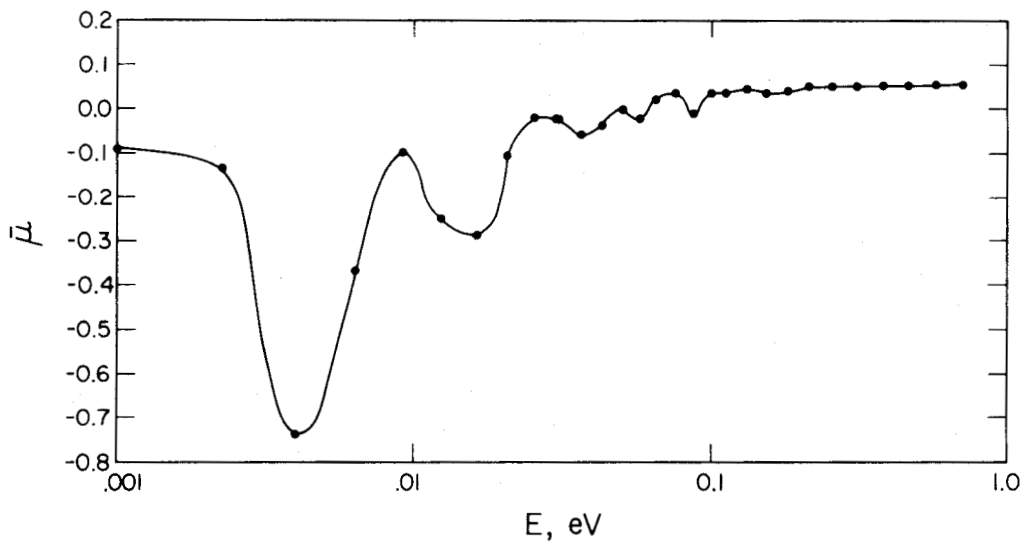


FIGURE 17 $\bar{\mu}$ as a Function of Energy for Beryllium Oxide at 296°K

The diffusion parameters obtained from the ENDF/B data for beryllium and beryllium oxide are compared to some experimental determinations in Tables X and XI. The PIDLE (ENDF/B) results for the room temperature diffusion constants are in excellent agreement with experiment. The large differences between the ENDF/B and experimental values for C in these tables may arise from the different buckling intervals used in the analyses. This possibility could not be adequately tested in the present calculations since the validity of the asymptotic flux assumption in PIDLE is questionable for the relatively large bucklings of the experiments. For room temperature beryllium and beryllium oxide, typical neutron mean free paths below the Bragg cutoffs, 0.006 and 0.004 eV, respectively, are in the range 15-20 cm. Because PIDLE uses a single Fourier component to represent the spatial dependence, calculations should be limited to systems having thicknesses greater than 2 mean free paths (~34 cm), i.e., systems with

$$B^2 < \left(\frac{\pi}{34}\right)^2 \approx .0085 \text{ cm}^2$$

In Figure 18, for example, the PIDLE results for $\lambda - \lambda_0$ for beryllium at 296°K are in excellent agreement with the measurements of Andrews³⁵ for $B^2 < 0.008 \text{ cm}^{-2}$, but the agreement deteriorates as the buckling increases.

TABLE X
Diffusion Parameters for Beryllium
($\rho = 1.84 \text{ g/cm}^3$)

Method	B^2 Interval	T, °K	$D_0, 10^5 \text{ cm}^2/\text{sec}$	C, $10^5 \text{ cm}^4/\text{sec}$
ENDF/B Data	$-0.001 < \Sigma_a < 0.001 \text{ cm}^{-1}$	296	1.27	18.3
		400	1.34	1.96
		500	1.47	1.18
		600	1.60	1.15
		700	1.73	1.19
		800	1.84	1.22
		1000	2.06	1.26
		1200	2.25	1.29
Reference 35	$0.003 < B^2 < 0.075 \text{ cm}^{-2}$	296	1.235 ± 0.013	2.80 ± 0.3
Reference 36	$0.008 < B^2 < 0.072 \text{ cm}^{-2}$	296	1.25 ± 0.06	1.40 ± 1.0
Reference 37	$0.003 < B^2 < 0.041 \text{ cm}^{-2}$	296	1.24 ± 0.04	3.90 ± 0.8

TABLE XI
Diffusion Parameters for Beryllium Oxide
($\rho = 3.0 \text{ g/cm}^3$)

Method	B^2 Interval	$T, \text{ }^\circ\text{K}$	$D_{O_2}, 10^5 \text{ cm}^2/\text{sec}$	$C, 10^5 \text{ cm}^4/\text{sec}$
ENDF/B Data	$-0.001 < \Sigma_a < 0.001 \text{ cm}^{-1}$	296	1.27	48.7
		400	1.39	5.09
		500	1.54	2.69
		600	1.69	2.39
		700	1.82	2.32
		800	1.95	2.28
		1000	2.19	2.21
		1200	2.39	2.12
Reference 38	$0.02 < B^2 < 0.04 \text{ cm}^{-2}$	296	1.18 ± 0.02	3.85 ± 0.08
Reference 39	$0.0028 < B^2 < 0.0245 \text{ cm}^{-2}$	296	1.33 ± 0.01	4.87 ± 0.58

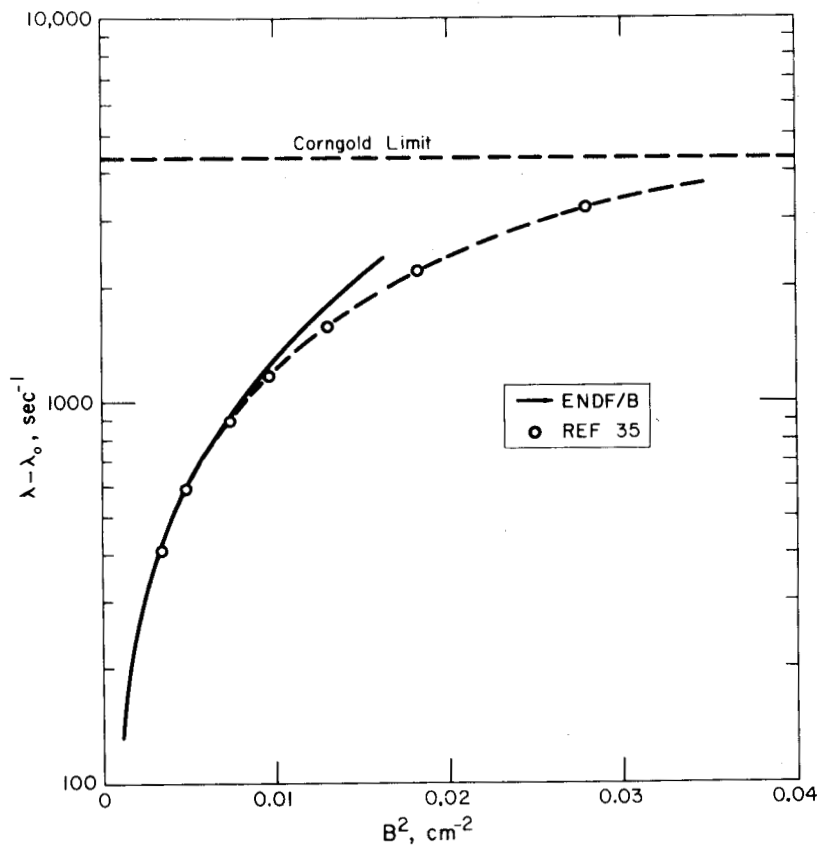


FIGURE 18 $\lambda - \lambda_0$ as a Function of B^2 for Beryllium at 296°K

Benzene

THERMOS scattering kernels were generated, tested, and found satisfactory at the following temperatures: 296°, 350°, 400°, 450°, 500°, 600°, 800°, and 1000°K. Figure 19 displays good agreement between the FLANGE II output for σ_T at 296°K and the measurements by Sprevak, et al.⁴⁰ The ENDF/B data is systematically lower than the measurements, but the differences are less than 2% of the total cross section. In contrast, the FLANGE II output yields values for \bar{u} which appear systematically higher than the measurements of Sprevak, et al. (Figure 20). These small differences serve to explain part of the 7% differences observed in Table XII between the ENDF/B diffusion constant at 296°K and the experimental determination by Kühle and Kussmal,⁴¹ but the magnitude of this difference between the ENDF/B and measured diffusion constants is surprising.

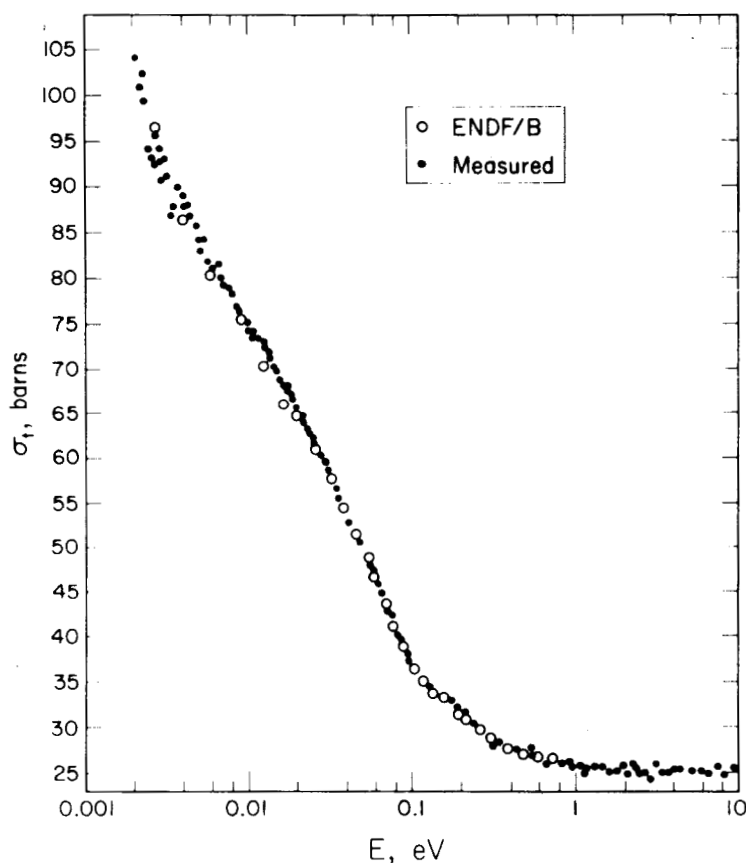


FIGURE 19 Total Neutron Cross Section for Benzene at 296°K

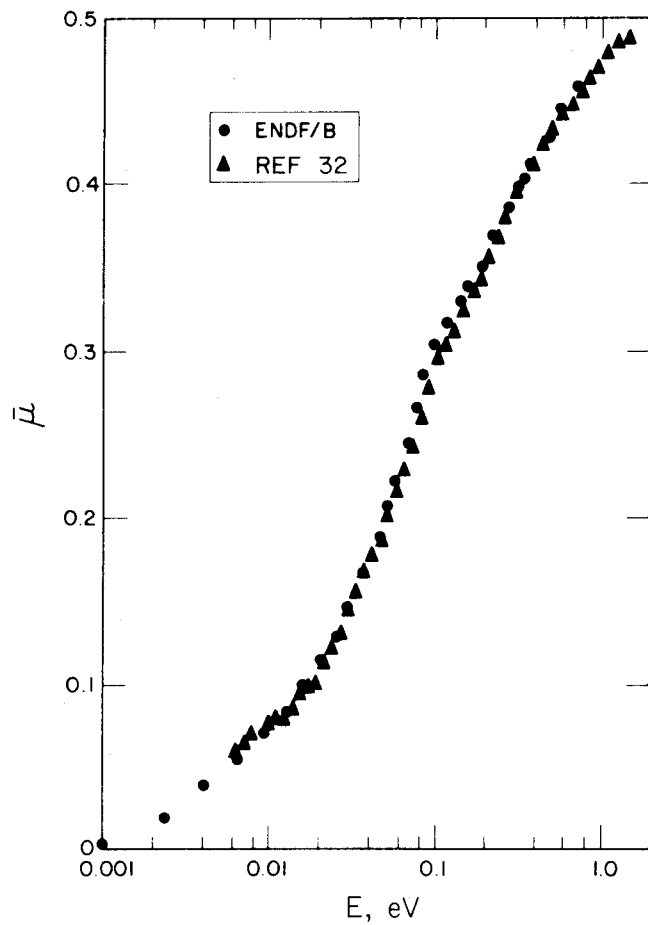


FIGURE 20 $\bar{\mu}$ as a Function of Energy for Benzene at 296°K

TABLE XII
Diffusion Parameters for Benzene
($\rho = 0.874 \text{ g/cm}^3$)

Method	$T, \text{ }^\circ\text{K}$	$D_0, 10^4 \text{ cm}^2/\text{sec}$	$C, 10^4 \text{ cm}^4/\text{sec}$
ENDF/B Data	296	5.26	1.95
	350	6.53	2.49
	400	7.03	2.33
	450	7.84	2.44
	500	9.11	2.88
	600	10.1	2.66
	800	13.6	3.30
	1000	15.2	3.04
Reference 41	296	4.85 ± 0.08	1.33 ± 0.24

Uranium Dioxide

THERMOS scattering kernels were generated at 296°, 400°, 500°, 600°, 700°, 800°, 1000°, and 1200°K. For all these temperatures, no unusual behavior was detected when the scattering cross section and $\bar{\mu}$ were plotted as a function of energy. The plots for room temperatures are shown in Figures 21 and 22. In contrast to the Bragg peaks traditionally observed in UO_2 transmission measurements (e.g., the analysis of Verdaguer, et al.⁴²), Figure 21 displays a smooth scattering cross section at thermal energies because in ENDF/B, elastic scattering has been computed in the incoherent approximation. No calculations of the diffusion parameters have been performed due to the sensitivity which such calculations have on the ^{235}U content.

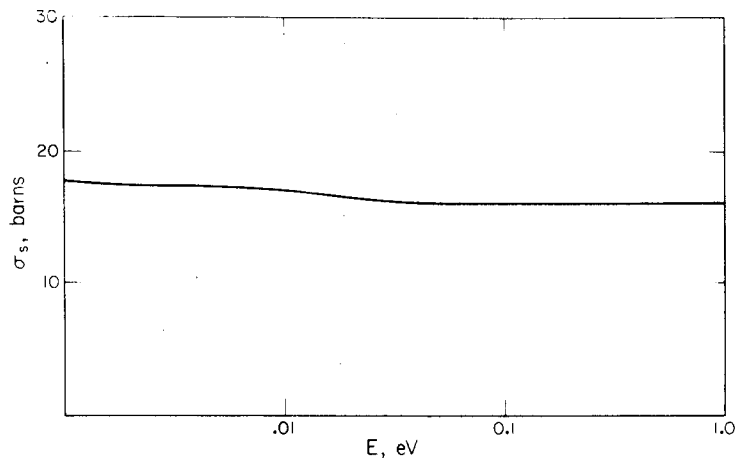


FIGURE 21 Scattering Cross Section for Uranium Dioxide at 296°K

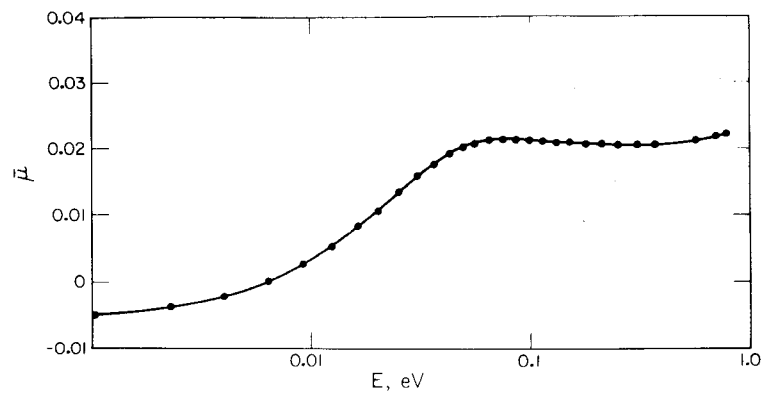


FIGURE 22 $\bar{\mu}$ as a Function of Energy for Uranium Dioxide at 296°K

APPENDIX

SCATTERING KERNEL LIBRARY AND RETRIEVAL ROUTINE

The scattering kernels generated to test the $S(\alpha,\beta,T)$ data on ENDF/B were made into a two-volume library on magnetic tape, and a retrieval routine was written to print and/or punch selected data from either volume. Group structure data for the kernels are included in each volume of the library. These kernel libraries and retrieval routines are available from the Argonne Code Center.

The retrieval routine provided with the tape library calls for one card of input for each kernel to be printed and/or punched. The format is as follows:

<u>Mnemonic</u>	<u>Column</u>	<u>Format</u>	<u>Description</u>
ZA	1-10	E10.0	ZA from Table II of desired kernel
T	11-20	E10.0	Temperature in °K of desired kernel
LEGØ	21-30	I10	Maximum Legendre orders desired for printing
NØPT	31-40	I10	Operation to be performed: =1 , punch kernel only =2 , print kernel only =3 , print and punch kernel
NT	41-50	I10	Data set on which tape volume is mounted

If ZA is specified as 0.0, the group structure in energy units will be printed.

As part of the retrieval package, a subroutine (named GETKER) is provided which may be included in a processing code to position tapes in front of selected kernels for direct reading into the processing code. Detailed usage of this routine is described by comments cards within the routine itself.

The structure of the kernel library tape volume is shown in Figure A-1.

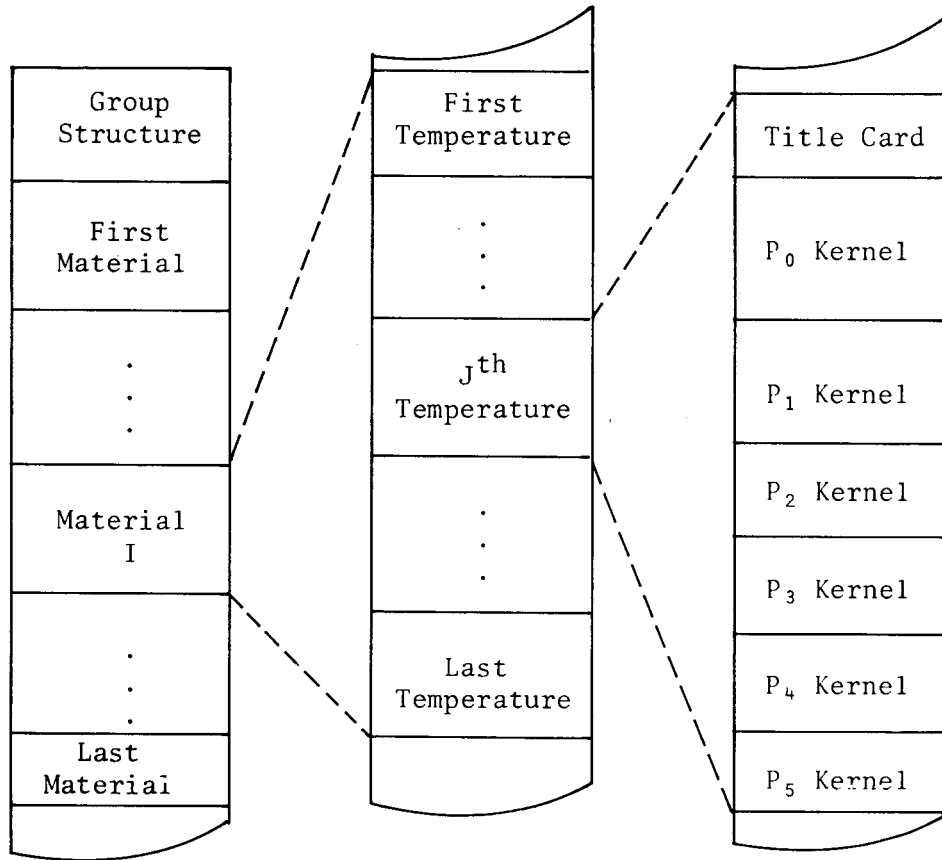


FIGURE A-1 Structure of Kernel Library Tape

All data on the kernel library is stored in BCD card image form. The formats for the various decks are described below.

GROUP STRUCTURE DECK

Card 1 -- Description Card

<u>Mnemonic</u>	<u>Column</u>	<u>Format</u>	<u>Description</u>
NG	1-10	I10	Number of groups
ELØW	11-20	E10.0	Low energy of group 1
(TITLE(I), I=1,13)	21-72	13A4	Description
NSEQ	79-80	I2	Card Sequence No.

Cards 2 – Group Characteristic Energies

<u>Mnemonic</u>	<u>Column</u>	<u>Format</u>	<u>Description</u>
(EC(I),I=1,7)	1-70	7E10.0	Characteristic energies of each group in order, eV
NT	78	I1	Card type identifier = 1
NSEQ	79-80	I2	Card Sequence No.

(Card 2 is repeated until all groups are complete.)

Cards 3 – Group Widths

<u>Mnemonic</u>	<u>Column</u>	<u>Format</u>	<u>Description</u>
(EB(I),I=1,7)	1-70	7E10.0	Energy width (eV) of each group in order
NT	78	I1	Card type identifier = 2
NSEQ	79-80	I2	Card Sequence No.

(Card 3 is repeated until all groups are complete.)

KERNEL DECK STRUCTURE

Card 1 – Title Card

72 alphanumeric characters. Columns 73-80 must be blank.

Card 1 is followed by from 1 to 6 kernel decks corresponding to P_0 through P_5 scattering kernels, respectively.

Card 2 – Kernel Header Card

<u>Mnemonic</u>	<u>Column</u>	<u>Format</u>	<u>Description</u>
LEGØ	1	I1	Legendre order of kernel
NGLØ	2-4	I3	Smallest group index in kernel
NEG	5-7	I3	Largest group index
T	9-20	E12.4	Temperature of kernel, °K

Cards 3 – Kernel Matrix Elements

<u>Field</u>	<u>Column</u>	<u>Format</u>	<u>Description</u>
1	1	I1	Legendre order 0-9
2	2-4	I3	Final energy group index (J) of the first word on this card
3	5-7	I3	Initial energy group index (I) of the data on this card
4	9-20	E12.4	σ_{ℓ} (I \rightarrow J)
5	21-32	E12.4	σ_{ℓ} (I \rightarrow J+1)
6	33-44	E12.4	σ_{ℓ} (I \rightarrow J+2)
7	45-56	E12.4	σ_{ℓ} (I \rightarrow J+3)
8	57-68	E12.4	σ_{ℓ} (I \rightarrow J+4)
9	69-76	F8.0	ZA designation of kernel
10	77-80	I4	Deck Sequence No.

Zero values are not loaded by Card 3, which presumes core has been cleared prior to loading kernels.

TL:mp

REFERENCES

1. H. C. Honeck and D. R. Finch. *FLANGE II, A Code to Process Thermal Neutron Data from an ENDF/B Tape*. USAEC Report DP-1278, Savannah River Laboratory, E. I. du Pont de Nemours & Co., Aiken, S. C. (1971).
2. J. U. Koppel. *Neutron Scattering by Hydrogeneous Moderators*. USAEC Report GA-7055, General Dynamics Corp., General Atomic Div., San Diego, Calif. (1966).
3. M. Nelkin. "The Scattering of Slow Neutrons by Water." *Phys. Rev.* 119, 741 (1960).
4. H. C. Honeck. "An Incoherent Thermal Scattering Model for Heavy Water." *Trans. Am. Nucl. Soc.* 5, 47 (1962).
5. A. Radkowsky. *Temperature Dependence of Thermal Transport Mean Free Path from Experimental Data on Scattering Cross Section of Water*. USAEC Report ANL-4476, Argonne National Laboratory, Argonne, Ill. (1950).
6. D. E. Parks, et al. "Neutron Spectra in Poisoned Graphite." *Trans. Am. Nucl. Soc.* 4, 135 (1961).
7. H. C. Honeck. "On the Calculation of Thermal Neutron Diffusion Parameters." *Proc. of the Brookhaven Conference on Neutron Thermalization*. USAEC Report BNL-719, Vol. IV, p 1186, Brookhaven National Laboratory, Upton, N. Y. (1962).
8. N. Corngold. "Some Transient Phenomena in Thermalization Theory." *Nucl. Sci. Eng.* 19, 80 (1964).
9. J. L. Russell, J. M. Neill, and J. R. Brown. *Total Cross Section Measurements of H₂O*. USAEC Report GA-7581, General Dynamics Corp., General Atomic Div., San Diego, Calif. (1966).
10. J. R. Beyster, et al. *Integral Neutron Thermalization, Annual Summary Report, October 1, 1965 through September 30, 1966*. USAEC Report GA-7480, General Dynamics Corp., General Atomic Div., San Diego, Calif. (1966).
11. E. Starr and J. Koppel. "Determination of Diffusion Hardening in Water." *Nucl. Sci. Eng.* 14, 224 (1962).

12. P. B. Parks, et al. "Thermal-Neutron Diffusion in Light and Heavy Water." *Nucl. Sci. and Eng.* 33, 209 (1968).
13. A. J. H. Goddard and P. W. Johnson. "Thermal-Neutron Diffusion in Aqueous Absorbing Solutions." *Nucl. Sci. Eng.* 37, 127 (1969).
14. N. P. Baumann. "Determination of Diffusion Coefficients for Thermal Neutrons in D₂O at 20, 100, 165, and 220°C." *Nucl. Sci. Eng.* 14, 179 (1962).
15. J. R. Beyster, et al. *Integral Neutron Thermalization, Annual Summary Report, October 1, 1964 through September 30, 1965.* USAEC Report GA-6824, General Atomic Corp., John Jay Hopkins Laboratory for Pure and Applied Science, San Diego, Calif. (1965).
16. D. J. Hughes and R. B. Schwarts. *Neutron Cross Sections.* USAEC Report BNL-325, Second Edition, Brookhaven National Laboratory, Upton, N. Y. (1958).
17. N. K. Ganguly and A. W. Waltner. "Measurement of Neutron Diffusion Parameters of Heavy Water at Different Temperatures by Pulsed Source Method." *Trans. Am. Nucl. Soc.* 4, 282 (1961).
18. B. K. Malaviya and A. E. Profio. "Measurements of the Diffusion Parameters of Heavy Water by the Pulsed-Neutron Technique." *Trans. Am. Nucl. Soc.* 6, 58 (1963).
19. G. Kussmaul and H. Meister. "Thermal Neutron Diffusion Parameters of Heavy Water." *J. Nucl. Eng., Parts A/B* 17, 411 (1963).
20. D. Spielberg. "Neutron Cross Sections of Deuterium and D₂O for Multigroup Calculations." *Trans. Am. Nucl. Soc.* 1, 155 (1958).
21. J. M. Neill, et al. *Graphite Interface Studies, Technical Summary Report, May 16, 1963 through September 30, 1965.* USAEC Report GA-6753, General Atomic Corp., John Jay Hopkins Laboratory for Pure and Applied Science, San Diego, Calif. (1965).
22. K. H. Beckurts and K. Wirts. *Neutron Physics.* Springer-Verlag, New York (1964), p. 389.

23. E. Starr and G. A. Price. *Measurement of the Diffusion Parameters of Graphite and Graphite-Bismuth by Pulsed Neutron Methods.* USAEC Report BNL-719, Vol. 3, Brookhaven National Laboratory, Upton, N. Y. (1962).
24. A. Takahashi and K. Sumita. "Pulse Propagation Experiments of Thermal Neutrons in Graphite." *J. Nucl. Sci. Tech.* 5, 7 (1968).
25. R. B. Perez and R. E. Uhrig. "Propagation of Neutron Waves in Moderating Media." *Nucl. Sci. Eng.* 17, 90 (1963).
26. G. M. Borgonovi, et al. *Integral Neutron Thermalization, Annual Summary Report, October 1, 1968 through September 30, 1969.* USAEC Report GA-9753, Gulf General Atomic, Inc., San Diego, Calif. (1969).
27. H. Antunez, et al. *Integral Neutron Thermalization, Quarterly Progress Report, for the period ending March 31, 1966.* USAEC Report GA-7091, General Dynamic Corp., General Atomic Div., San Diego, Calif. (1966).
28. W. Gläser. "Untersuchungen der unelastischen Streuung langsamer Neutronen an Moderatoren." *Nukleonik* 11, 282 (1968).
29. W. Reichardt. "Thermalization of Neutrons in Zirconium Hydride and Ice." *Neutron Thermalization and Reactor Spectra, Vol. 2*, p. 411, IAEA, Vienna (1968).
30. J. W. Meadows and J. F. Whalen. "Thermalization and Diffusion Parameters of Neutrons in Zirconium Hydride." *Nucl. Sci. Eng.* 13, 230 (1961).
31. S. B. Armstrong. "The Energy-Dependent Total Neutron Cross Section of Polyethylene." *Nucl. Sci. Eng.* 23, 192 (1965).
32. J. R. Beyster, et al. *Angular Scattering by CH₂, ZrH_{1.85}, and C₆H₆.* USAEC Report GA-8030, General Dynamics Corp., General Atomic Div., San Diego, Calif. (1967).
33. N. G. Sjöstrand, J. Medinis, and T. Nilsson. "Geometric Buckling Measurements Using the Pulsed Neutron Source Method." *Arkiv För Fysik* 15, 471 (1959).
34. E. Fermi, W. J. Sturm, and R. G. Sachs. "The Transmission of Slow Neutrons through Microcrystalline Materials." *Phys. Rev.* 71, 589 (1947).

35. W. M. Andrews. *Measurement of the Temperature Dependence of Neutron Diffusion Properties in Beryllium Using a Pulsed Neutron Technique.* USAEC Report UCRL-6083, University of California, Lawrence Radiation Laboratory, Livermore, Calif. (1960).
36. G. De Saussure and E. G. Silver. *Determination of the Neutron Diffusion Parameters in Room-Temperature Beryllium.* USAEC Report ORNL-2641, Oak Ridge National Laboratory, Oak Ridge Tenn. (1959).
37. T. T. Komoto and F. Kloverstrom. "Diffusion Cooling in Beryllium and Graphite." *Trans. Am. Nucl. Soc.* 1, 94 (1958).
38. S. B. D. Iyengar, G. S. Mani, R. Ramanna, and N. Umakanta. *Proc. Indian Acad. Sci.* 45, 215 (1957).
39. B. V. Joshi, V. R. Nargundkar, and K. Subbarao. "Diffusion Parameters of BeO by Pulsed Neutron Method." *J. Nucl. Eng., Parts A/B* 19, 515 (1965).
40. D. Sprevak, et al. *Neutron Thermalization in Benzene.* USAEC Report GA-8185, General Dynamics Corp., General Atomic Div., San Diego, Calif. (1967).
41. M. Kuchle and G. Kussmaul. "Messung de Neutronen-Diffusionsparameter von Benzol mit der Impulsmethode." *Nukleonik* 6, 329 (1964).
42. F. Verdaguer, et al. "Diffraction des neutrons lents par les poudres microcristallines d' UO_2 et de CeO_2 ." *Helv. Phys. Acta* 25, 79 (1952).

